Thermodynamic Difference Rules: A Prescription for Their Application and Usage to Approximate Thermodynamic Data†

H. Donald Brooke Jenkins*,‡ and Leslie Glasser*,§

Department of Chemistry, University of Warwick, Coventry, West Midlands CV4 7AL, United Kingdom, and Nanochemistry Research Institute, Department of Chemistry, Curtin University of Technology, Perth 6845, Western Australia

Thermodynamic data are required for an understanding of the behavior of materials but are often lacking (or even unreliable) for a variety of reasons such as synthetic problems, purity issues, failure to correctly identify hydrolysis products, instability of the material, etc. Thus, it is necessary to develop procedures for the estimation of that data. The Thermodynamic Difference Rules (TDR) are additive approximations by which the properties of materials are estimated by reference to those of related materials. These rules appear in the form of the reliable Hydrate Difference Rule (HDR), based on the well-established properties of the large number of known hydrates, and the somewhat less certain Solvate Difference Rule (SDR). These rules are briefly surveyed and their application carefully delineated by a scheme and demonstrated by a number of calculated examples.

Introduction

It must be admitted that thermodynamic properties,[1] although useful, are frequently unavailable for the materials of importance in modern chemistry. Over three decades ago, O'Hare[2] drew attention to this shortfall of data when he noted that *high-tech* materials often have *low-tech* thermodynamics. The situation, far from improving, seems to have become even worse. Yet, in a climate of increasing demands on scientific resources worldwide, the prospect of the routine experimental determination of the key thermodynamic properties (i.e., $\Delta_f G°$, $\Delta_f H°$, and $S°_{298}$)—much in the manner by which provision of crystallographic data is standard practice for newly synthesized materials—is unlikely to emerge on any foreseeable future scientific agenda. A convenient route out of this difficulty has seemed to us to devise procedures which could estimate thermodynamic data either relying on existing known thermodynamic information or derived from readily available *crystallographic* databases. The former development gave rise to the Thermodynamic (Hydrate and Solvate) Difference Rules (TDR),[3–7] while the latter has resulted in our Volume-Based Thermodynamics (VBT) procedures[8–20] (consideration of which will be deferred to a subsequent publication[21]).

These two approaches are gradually being adopted, the former (TDR) to provide data for modern synthetic reactions taking place within nonaqueous media[7] and the latter (VBT) to provide a whole range of applications in areas where no thermodynamic data are otherwise available. Some progress *is* currently being made toward the expansion of the thermodynamic property database, but increasingly, this is not from experimental sources. Instead, data are being provided by quantum chemical calculations[22–27] and by empirical[28–31] and group contribution methods[32–34]—where we have simply noted just a few representative examples. Papers reporting thermochemical data based solely on calorimetric measurements are proportionately fewer with time, contrasted with the increasing proportion of those emerging from quantum chemical and other theoretical methods, of one variety or another.

We review briefly our contributions through the Thermodynamic Difference Rules, which are forms of the additivity rule. They comprise a rule for hydrate salts (the Hydrate Difference Rule, HDR) which works very satisfactorily and a rule for inorganic solvate systems, more generally, the Solvate Difference Rule (SDR), currently still very much under development. The latter rule is subject to greater uncertainties pending further data generation by experimental or other means. Indeed, Fyfe et al.[35] have earlier noted that "... if both heats and entropies were exactly additive, [Gibbs] energies would also be additive, and the [Gibbs]-energy change for any reaction between such compounds should be zero... More generally, if the additivity rule were exactly obeyed, all phases would always be in equilibrium...".

We provide a flow-chart (Scheme 1) enabling these TDR procedures to be easily understood and used by occasional users and nonexperts wishing to introduce, perhaps for the first time, thermodynamic arguments in support of their results.

Our procedures are such that they can also be used to provide speculative thermodynamic data for hypothetical, as yet unprepared, materials as well as for those that are challenging to handle experimentally, being unstable, radioactive, or hygroscopic.

Thermodynamic Difference Rule (TDR) Procedures. In its most important role, the TDR[3–7] is designed to provide a means whereby new thermodynamic data can be inferred from established data. We examine its credentials by considering separately the hydrate ($M_pX_q \cdot nH_2O$) and solvate ($M_pX_q \cdot nS$) difference rules. We list and examine the use of various relationships which we have developed and demonstrate their use both for the validation of existing data when choices are possible and in checking the consistency of data sets.

† Part of the "Sir John S. Rowlinson Festschrift".

* Corresponding authors. H. D. B. Jenkins. E-mail: h.d.b.jenkins@warwick.ac.uk. Telephone: +44 2476-523-265 or +44 2476-466-747. Fax: + 44 2476-524-112 or +44 2476-466-747. L. Glasser. E-mail: l.glasser@curtin.edu.au. Telephone: + 61 8 9266-3126. Fax: + 61 8 9266-4699.
‡ University of Warwick.
§ Curtin University of Technology.

10.1021/je100383t
Published on Web 06/14/2010

Scheme 1

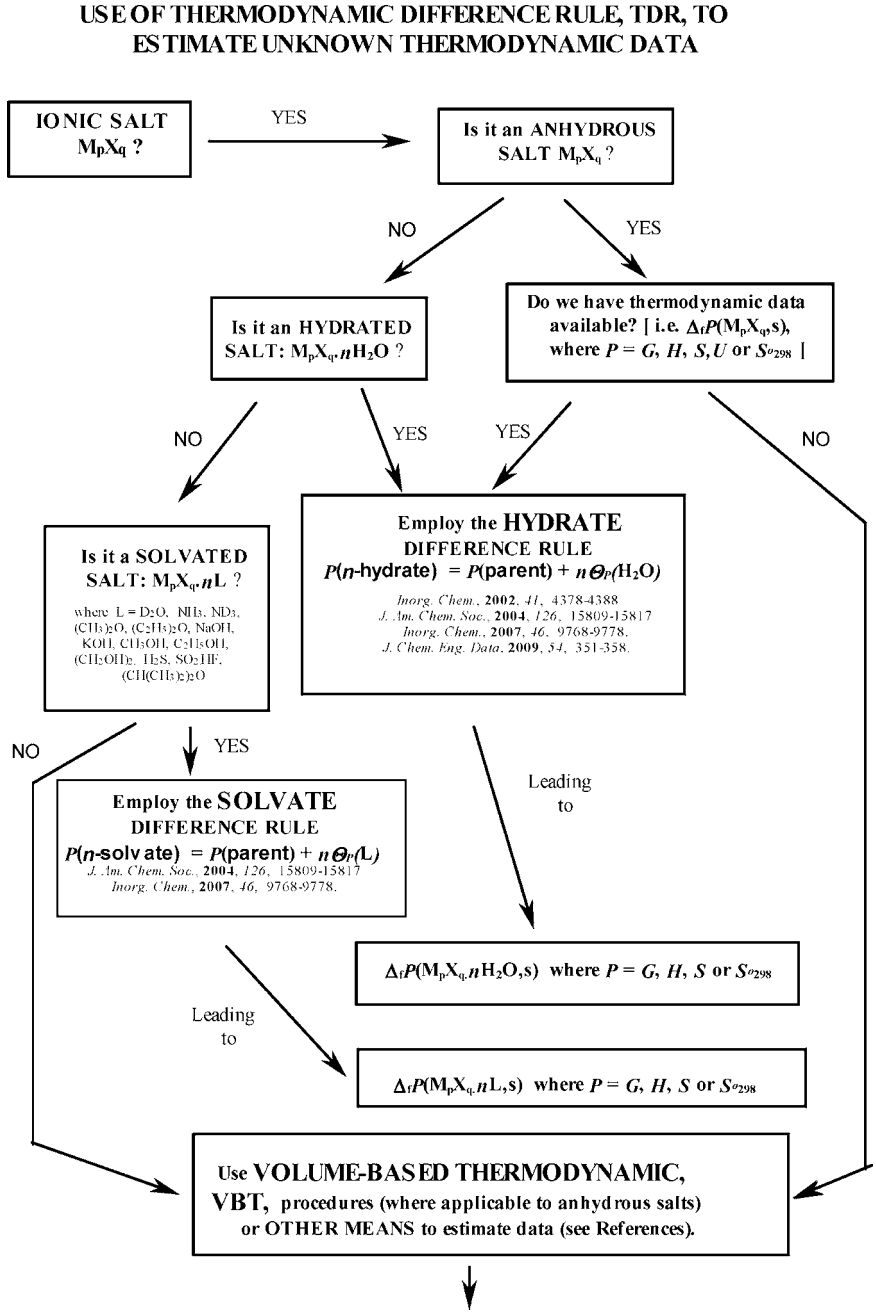

This paper simplifies notation wherever possible. More details can be found in the main papers,[3–6] while Table 1 provides the key.

$$P(n\text{-hydrate}) \approx P(\text{parent}) + n\theta_P(H_2O) \quad (1)$$

$$[P(m\text{-hydrate}) - P(n\text{-hydrate})] \approx (m\text{-}n)\theta_P(H_2O) \quad (2)$$

$$P(k\text{-hydrate}) + P(l\text{-hydrate})] \approx P(m\text{-hydrate}) + P(n\text{-hydrate}) \quad \text{with } k + l = m + n \quad (3)$$

$$P(k\text{-hydrate}) + P(l\text{-hydrate}')] \approx P(m\text{-hydrate}) + P(n\text{-hydrate}') \quad \text{with } k + l = m + n \quad (4)$$

where these equations, which are simply variations of one another, are expressions of the additivity of corresponding thermodynamic properties, as defined in Table 1, top of third column. Equation 2 follows directly from eq 1.

θ_P values are reasonably constant throughout for all hydrates (whether single or complex), with the values being well established for the standard thermodynamic properties: $\Delta_f H°$, $\Delta_f G°$, and $S°_{298}$.

$$\theta_{Hf}(H_2O)/\text{kJ}\cdot\text{mol}^{-1} \approx -298.6 \quad (5)$$

$$\theta_{Gf}(H_2O)/\text{kJ}\cdot\text{mol}^{-1} \approx -242.4 \quad (6)$$

$$\theta_S(H_2O)/\text{J}\cdot\text{K}^{-1}\cdot\text{mol}^{-1} \approx 40.9 \quad (7)$$

Usage of HDR Equations

Usage is illustrated by several practical examples.

Example 1: Standard Entropy Estimation. The NBS database[36] lists the standard entropy for copper sulfate monohydrate, $S°_{298}(CuSO_4\cdot H_2O, s)/\text{J}\cdot\text{K}^{-1}\cdot\text{mol}^{-1}$, to be 146.0. Predict the standard entropies, $S°_{298}(CuSO_4\cdot nH_2O,s)$, of the *3*, *5*, and *6* hydrates and of the parent, $S°_{298}(CuSO_4,s)$.

From eq 1, using $\theta_S(H_2O)$ from eq 7, $S°_{298}(n\text{-hydrate}) \approx S°_{298}(\text{parent}) + 40.9n$, so, rearranging, we predict that

Table 1. Simplified Notation Used in the Current Paper

full notation as used in main papers[3–6]	notation adopted here	interpretation
$P(M_pX_q, s)$	$P(\text{parent}) \equiv P(0\text{-hydrate})$	P represents the thermodynamic property under consideration, which may be standard enthalpy of formation, Gibbs energy of formation, or standard entropy.
$P(M_pX_q \cdot nH_2O, s)$	$P(n\text{-hydrate})$	
$P(M'_pX'_q \cdot nH_2O, s)$	$P(n\text{-hydrate}')$	
$P(M_pX_q \cdot nL, s)$	$P(n\text{-solvate})$	
$P(M'_pX'_q \cdot nL, s)$	$P(n\text{-solvate}')$	M_pX_q represents an inorganic salt in the crystalline state (s).
$P(M'_pX'_q, s)$	$P(\text{parent}') \equiv P(0\text{-hydrate}')$	$M'_pX'_q$ represents a different inorganic salt, distinguishable from M_pX_q. Unsolvated/anhydrous materials are distinguished as parent and parent′. L represents a nonaqueous solvent. H_2O represents specifically water.
$\theta_P(H_2O, \text{s-s})$	$\theta_P(H_2O)$	θ_P represents a constant property contribution whose value is appropriate to the property P being investigated, the solvent L involved (water for hydrates), and the physical states of the solvate/hydrate and parent salts considered, most usually solids (s), hence s-s.
	$\theta_{Hf}(H_2O)/\text{kJ}\cdot\text{mol}^{-1} \approx -298.6$ $\theta_{Gf}(H_2O)/\text{kJ}\cdot\text{mol}^{-1} \approx -242.4$ $\theta_S(H_2O)/\text{J}\cdot\text{K}^{-1}\cdot\text{mol}^{-1} \approx 40.9$	$\theta_{Hf}(H_2O)$ and $\theta_{Gf}(H_2O)$ refer to the specific θ value used when considering standard enthalpies of formation, $\Delta_fH°$, and Gibbs energies of formation, $\Delta_fG°$, respectively. $\theta_S(H_2O)$ refers to the property of standard entropy, $S°_{298}$, of water.
$\theta_P(L, \text{s-s})$	$\theta_P(L)$	Values for $\theta_P(L)$ for a limited number of solvents, L, and properties P are listed in Table 1 of ref 4.

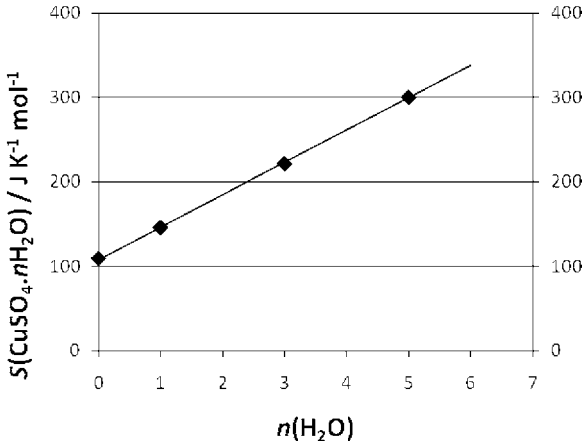

Figure 1. HDR of $S°_{298}(n\text{-hydrate, s})$ for $CuSO_4$ versus $n(H_2O)$. The least-squares fitted line has the equation $S°_{298}(n\text{-hydrate, s})/\text{J}\cdot\text{K}^{-1}\cdot\text{mol}^{-1} \approx 38.2n + 108.3$ ($R^2 = 0.9998$, $N = 4$).

$$S°_{298}(CuSO_4, s)/\text{J}\cdot\text{K}^{-1}\cdot\text{mol}^{-1} \approx 146.0 - 40.9 = 105.1\ (109.3 \pm 0.4^{37}\ 3.8\ \%)$$

$$S°_{298}(CuSO_4\cdot 3H_2O, s)/\text{J}\cdot\text{K}^{-1}\cdot\text{mol}^{-1} \approx 227.8\ (221.3,\ 2.9\ \%)$$

$$S°_{298}(CuSO_4\cdot 5H_2O, s)/\text{J}\cdot\text{K}^{-1}\cdot\text{mol}^{-1} \approx 309.6\ (300.4,\ 3.1\ \%)$$

and

$$S°_{298}(CuSO_4\cdot 6H_2O, s)/\text{J}\cdot\text{K}^{-1}\cdot\text{mol}^{-1} \approx 350.5$$

Comparison with experimental values (in parentheses), known for $n = 3$ and 5, leads to the errors listed. $S°_{298}(CuSO_4\cdot 6H_2O, s)/\text{J}\cdot\text{K}^{-1}\cdot\text{mol}^{-1}$ has not been recorded, and this prediction should be good to (approximately) $\pm$ 15 $\text{J}\cdot\text{K}^{-1}\cdot\text{mol}^{-1}$. It should be mentioned that, if one is wishing to predict a value for a hydrate within a family of hydrates *for which experimental values are known for several members of the series*, then the preferred route would be to plot the specific experimental $P(n\text{-hydrate, s})$ values.

Thus, for the $n = 0$, 1, 3, and 5 hydrates, a plot of $S°_{298}(CuSO_4\cdot nH_2O, s)/\text{J}\cdot\text{K}^{-1}\cdot\text{mol}^{-1}$ versus n leads (Figure 1) to eq 8 from which we can predict a more likely hexahydrate entropy, based on the series concerned rather than the general θ values

$$S°_{298}(CuSO_4\cdot nH_2O, s)/\text{J}\cdot\text{K}^{-1}\cdot\text{mol}^{-1} \approx 38.2n + 108.3 \quad (R^2 = 0.9998, N = 4) \quad (8)$$

$$S°_{298}(CuSO_4\cdot 6H_2O, s)/\text{J}\cdot\text{K}^{-1}\cdot\text{mol}^{-1} \approx 337.5$$

An approximate hydrate entropy value can also be estimated using Latimer's additive approach,[38,39] from which $S°_{298}(CuSO_4\cdot 6H_2O, s)/\text{J}\cdot\text{K}^{-1}\cdot\text{mol}^{-1} \approx 45.2 + 72.0 + 6(39.3) = 353.2$.

Example 2: Gibbs Energy Estimation. The NBS database[36] lists the standard Gibbs energy of formation, $\Delta_fG°$, for the parent and three hydrates of $ZnSO_4\cdot nH_2O$ (Table 2). Using the end members ($n = 0$ and 7), use eq 2 to estimate $\theta_{Gf}(H_2O)/\text{kJ}\cdot\text{mol}^{-1}$. (Our generic value, eq 6, is -242.4 $\text{kJ}\cdot\text{mol}^{-1}$.)

Table 2. Gibbs Energy of Formation, $\Delta_fG°$, for the Parent and Three Hydrates of $ZnSO_4\cdot nH_2O$

n	0	1	6	7
$\Delta_fG°/\text{kJ}\cdot\text{mol}^{-1}$	−871.5	−1131.99	−2324.44	−2562.67

Using eq 2 ($P = \Delta_fG°$) and the end members

$$\theta_{Gf}(H_2O)/\text{kJ}\cdot\text{mol}^{-1} \approx [P(7\text{-hydrate}) - P(\text{parent})]/(7 - 0) = [-2562.67 + 871.5]/7 = -241.6\ (0.3\ \%)$$

A more suitable alternative strategy is to plot the data versus n, as shown in Figure 2. The linear fit takes the analytical form

$$\Delta_fG°(n\text{-hydrate, s})/\text{kJ}\cdot\text{mol}^{-1} \approx -240.6n - 880.7\ (R^2 = 0.999, N = 4) \quad (9)$$

from which we infer for $ZnSO_4$ hydrates that

$$\theta_{Gf}(H_2O)/\text{kJ}\cdot\text{mol}^{-1} \approx -240.6\ (0.8\ \%)$$

Example 3. Example 3 shows that the experimental data for $ZnSO_4$ hydrate in Table 2 above fits eq 3 under the condition that $k + l = m + n$.

Taking $k = 0$, $l = 7$, $m = 1$, and $n = 6$, satisfying the condition, the data show that

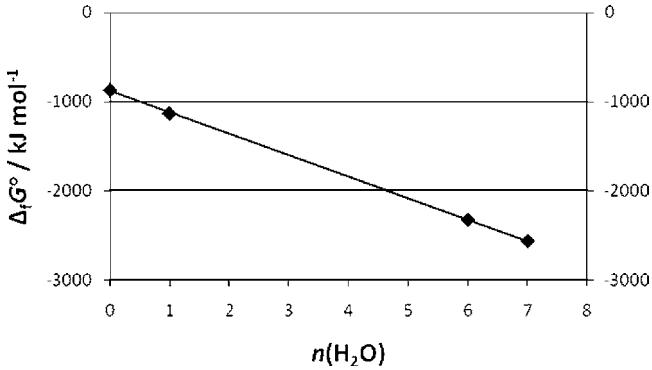

Figure 2. HDR of $\Delta_f G°$(*n*-hydrate, s)/kJ·mol^{-1} for $ZnSO_4$ versus $n(H_2O)$. The least-squares fitted line has the equation $\Delta_f G°$(*n*-hydrate, s)/J·K^{-1}·mol^{-1} = −240.6*n* − 880.7 (R^2 = 0.999, N = 4).

Table 3. Enthalpies of Formation, $\Delta_f H°$, for the Parents and Hydrates of $MgSO_4$ and of $MgSeO_4$, from Different Sources

$\Delta_f H°$(*n*-hydrate, s) kJ·mol^{-1}	K&K[40,42,43]	K&K[40,42,44]	NBS[36]
$MgSO_4$	−1301.43	−1301.43	−1284.9
$MgSO_4·H_2O$	−1278.2	−1604.6	−1602.1
$MgSO_4·1.25H_2O$	−1673.2	−1671.1	
$MgSO_4·1.5H_2O$	−1753.5	−1748.5	
$MgSO_4·2H_2O$	−1953.9	−1943.9	−1896.2
$MgSO_4·3H_2O$	−2210.4	−2200.8	
$MgSO_4·4H_2O$	−2530.9	−2520	−2496.6
$MgSO_4·5H_2O$			−2795.75
$MgSO_4·6H_2O$	−3104.1	−3084.4	−3087
$MgSO_4·7H_2O$	−3376.5	−3366.9	−3388.7
$MgSeO_4$	−983.32	−999	−968.5
$MgSeO_4·H_2O$	−1312.43	−1310.26	−1295.45
$MgSeO_4·4H_2O$	−2204.47	−2204.8	−2189.91
$MgSeO_4·6H_2O$	−2835.41	−2793.9	−2779

Table 4. Optimized Enthalpies of Formation, $\Delta_f H°$, for the Parents and Hydrates of $MgSO_4$ and of $MgSeO_4$, Using the Different Sources for Reference

sum of squares of errors	96844	3019	661
	% diff K&K[40,42,43]	% diff K&K[40,42,44]	% diff NBS[36]
$MgSO_4$	4.3	−0.8	−0.7
$MgSO_4·H_2O$	−21.7	−0.2	0.5
$MgSO_4·1.25H_2O$	2.4	−0.7	(−1668.4)[a]
$MgSO_4·1.5H_2O$	2.5	−0.5	(−1743.3)[a]
$MgSO_4·2H_2O$	4.6	2.0	0.2
$MgSO_4·3H_2O$	1.6	0.0	(−2193.1)[a]
$MgSO_4·4H_2O$	1.9	0.9	0.1
$MgSO_4·5H_2O$	–	–	0.1
$MgSO_4·6H_2O$	0.0	−0.2	−0.2
$MgSO_4·7H_2O$	−1.1	−0.6	−0.1
$MgSeO_4$	0.0	−1.2	−1.6
$MgSeO_4·H_2O$	1.5	0.2	0.9
$MgSeO_4·4H_2O$	−0.7	0.3	0.3
$MgSeO_4·6H_2O$	−0.2	0.1	−0.1

[a] The formation enthalpies in parentheses are calculated for the missing entries in the NBS tables.

$$[P(k\text{-hydrate}) + P(l\text{-hydrate})]/\text{kJ·mol}^{-1} = [P(0\text{-hydrate}) + P(7\text{-hydrate})] = -3434.2$$

and that

$$[P(l\text{-hydrate}) + P(m\text{-hydrate})]/\text{kJ·mol}^{-1} = [P(1\text{-hydrate}) + P(6\text{-hydrate})] = -3456.4$$

and hence that, to within 0.6 %, eq 3 is valid.

Example 4: Consistency Check of Data. The NBS[36] and Karapet'yants and Karapet'yants[40–43] tabulations cite differing values for the $MgSO_4$ and $MgSeO_4$ parent and hydrate enthalpies, as in Table 3. We investigate which set of data is most self-consistent.

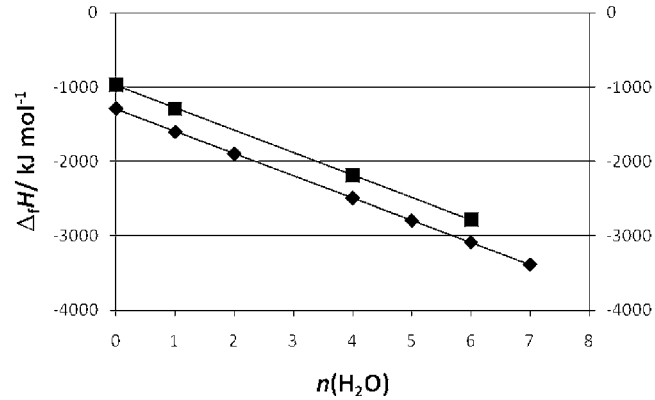

Figure 3. HDR of $\Delta_f H°$(*n*-hydrate, s)/kJ·mol^{-1} for $MgSO_4$ and its hydrates (diamonds) and $MgSeO_4$ and its hydrates (squares) versus $n(H_2O)$. The slopes of linear plots are (−299.5 and −298.8) kJ·mol^{-1}, respectively.

Table 4 shows the results of application of the Excel "Solver" optimization routine (see Supporting Information) using the columns of enthalpy data from the table above and allowing Solver to optimize simultaneously the enthalpy contributions of H_2O, $MgSO_4$, and $MgSeO_4$. (Solver operates in this instance by minimizing the sum-of-squares difference between the literature formation enthalpies and those calculated from a starting set of enthalpies for the component species (H_2O, $MgSO_4$, and $MgSeO_4$), by adjusting the latter values.) Quite clearly, the NBS data set is most suitable, with $\Delta_f H°(H_2O, s) = -299.9$, $\Delta_f H°(MgSO_4, s) = -1293.6$, and $\Delta_f H°(MgSeO_4, s) = -983.6$ kJ mol^{-1}.

From Figure 3, the slopes of enthalpy versus $n(H_2O)$ linear plots are −299.4 and −298.8 kJ·mol^{-1}, for $MgSO_4$ and $MgSeO_4$ hydrates, respectively, compared with the best optimized value of −299.9 kJ·mol^{-1} noted above, and the generalized value of $\theta_{Hf}(H_2O) = -298.6$ kJ·mol^{-1} from eq 5.

Example 5: Do the Hydrates Formed by Salts of Organic Acids Obey the Difference Rule? The number of hydrate examples of organic acids for which thermodynamic data are available is somewhat limited. To examine this question, in Table 5 we cite examples of $\Delta_f H°$ for some organic acid salts as given in the NBS tables[36] and use the Thermodynamic Difference Rule, taking $\theta_{Hf}(H_2O, s\text{-}s) = -298.6$ kJ·mol^{-1} to predict the hydrate value from the given parent entry. The final column shows the % error, from which we see that the rule does enable estimation of this data, usually to within experimental error.

HDR Errors. Experimental values[36,40] for $\Delta_f G°(MgSO_4·6H_2O,s)$/kJ·mol^{-1}, to take an example of a typical hydrate, exhibit a range of 21 kJ·mol^{-1} (a range of 1 %), from −2603.7 to −2628.64. This degree of uncertainty is often comparable with the errors arising from HDR predictions, rendering the latter extremely useful. In our previous studies, it was recorded that $\Delta_f G°$ was predicted to within less than 1 % of the accepted value in 88 % of cases.

Solvate Difference Rule (SDR).

$$P(n\text{-solvate}) \approx P(\text{parent}) + n\theta_P(\text{L}) \quad (10)$$

$$[P(m\text{-solvate}) - P(n\text{-solvate})] \approx (m - n)\theta_P(\text{L}) \quad (11)$$

$$P(k\text{-solvate}) + P(l\text{-solvate})] \approx P(m\text{-solvate}) + P(n\text{-solvate}) \quad (12)$$

and more detailed rules involving change of parent and/or solvent

$$P(M_pX_q\cdot kL,s) + P(M'_pX'_q\cdot lL',s) \approx P(M_pX_q\cdot lL',s) + P(M'_pX'_q\cdot kL,s) \quad (13)$$

$$P(M_pX_q\cdot kL,s) + P(M'_pX'_q,s) \approx P(M_pX_q,s) + P(M'_pX'_q\cdot kL,s) \quad (14)$$

$$P(M_pX_q\cdot kL,s) + P(M'_pX'_q\cdot lL,s) \approx P(M_pX_q\cdot mL,s) + P(M'_pX'_q\cdot nL,s) \quad (15)$$

Further, if L′ is specifically H_2O, then

$$P(M_pX_q\cdot kL,s) + P(M'_pX'_q\cdot lH_2O,s) \approx P(M_pX_q\cdot lH_2O,s) + P(M'_pX'_q\cdot kL,s) \quad (16)$$

where eq 11 derives directly from eq 10. In eqs 12 and 15, the condition $k + l = m + n$ must hold.

There are several general observations to be made at the outset with regard to $\Delta_fH°$, $\Delta_fG°$, and $S°_{298}$ data for nonaqueous solvates, $M_pX_q\cdot nL$:

(1) Thermodynamic data available for solvates are generally sparse;

(2) Multiple determination of identical thermodynamic data is infrequent (so errors are difficult to quantify). This is an area which could do with further experimental work.

(3) Often, only $\Delta_fH°(M_pX_q\cdot nL, s)$ experimental values are available[6] (e.g., for solvents L = D_2O, $(C_2H_5)_2O$, NaOH, CH_3OH, C_2H_5OH, $(CH_2O)_2$, H_2S, and SO_2) and then often for very few compounds (3, 4, 3, 5, 11, 4, 4, and 9 respectively, for the solvents listed). Even with such limited data, correlation coefficients tend to be large, suggesting that SDR does apply.

(4) In very few cases (L = NH_3, ND_3, $(CH_3)_2O$) are experimental values of $\Delta_fG°(M_pX_q\cdot nL, s)$ and $S°_{298}(M_pX_q\cdot nL, s)$ available and then in limited numbers, (4, 3, and 3) and (9, 3, and 3), respectively.

All of these factors lead to the result that the SDR is less accurate than the HDR in its predictions: HDR correlation coefficients are generally high, with large numbers of data sets (for $\Delta_fH°$, $R^2 = 0.999$, $N = 342$; for $\Delta_fG°$, $R^2 = 0.998$, $N = 93$; and for $S°_{298}$, $R^2 = 0.978$, $N = 83$), while those for SDR are generally much lower—even for L = NH_3, for which there are 270 ammoniates for which $\Delta_fH°$ has been experimentally determined, the correlation coefficient is $R^2 = 0.932$. Having said this though, statistics does tell us that the probability that this correlation is due simply to chance is less than one in a million! Still, circumspection is the order of the day with regard to the use of SDR, as the following examples reveal.

Usage of SDR Equations

Example 6. There is considerable uncertainty concerning the formation enthalpies of the indium trihalides, as follows: $\Delta_fH°(InX_3, s)/kJ\cdot mol^{-1}$ for which values are −527.2,[40] −537.2[36] (X = Cl); −418.4,[40] −428.9[36] (X = Br); and −248.9,[40] −238.0[36] (X = I). We investigate the application of these SDR data to the indium trihalide *ammoniates*, using the data in Table 6 below.

In accordance with eqs 10 and 11, a plot is made of $P(n\text{-solvate})$ versus $n(NH_3)$ using the data displayed in Table 6. Figure 4 shows this plot where the linear analytical fits take the forms below (correlation coefficients in parentheses)

$$\Delta_fH°(InCl_3\cdot nNH_3,s)/kJ\cdot mol^{-1} = -92.10n - 622.7 \quad \text{(Diamonds, } R^2 = 0.985)$$

$$\Delta_fH°(InBr_3\cdot nNH_3,s)/kJ\cdot mol^{-1} = -94.22n - 518.6 \quad \text{(Squares, } R^2 = 0.985)$$

$$\Delta_fH°(InI_3\cdot nNH_3,s)/kJ\cdot mol^{-1} = -90.70n - 344.3 \quad \text{(Triangles, } R^2 = 0.988)$$

giving rise to an average value for $\theta_{Hf}(NH_3)$ of

$$\theta_{Hf}(NH_3)/kJ\cdot mol^{-1} \approx -92.3$$

which is some 14 % different than our global value of −105.5 $kJ\cdot mol^{-1}$ cited in Table 1 of ref 4 but exactly matches the minimum incorporation enthalpy more recently observed.[44] It should be noted that the intercepts give poor representation of the $\Delta_fH°(InX_3,s)/kJ\cdot mol^{-1}$ values. Errors here are 16 % (X = Cl), 21 % (X = Br), and 45 % (X = I).

This deserves some comment. The selection of only indium trihalide data for these specific plots would have been expected to provide a more appropriate value for $\theta_{Hf}(NH_3)$—optimized

Table 5. Formation Enthalpies of Organic Acid Salts and Their Hydrates, Predicted Enthalpies of Their Hydrates, and Percentage Errors

organic acid salt and hydrate(s)	$\Delta_fH°$ / $kJ\cdot mol^{-1}$	value predicted from the difference rule = parent value + $n\theta_{Hf}(H_2O, s\text{-}s)$	% error
	Bioxalate Salts and Double Oxalate Salts		
$NaHC_2O_4$ (s)	−1082.0		
$NaHC_2O_4\cdot H_2O$ (s)	−1384.1	−1380.6	0.2
$KHC_2O_4\cdot H_2C_2O_4$ (s)	−1951.0		
$KHC_2O_4\cdot H_2C_2O_4\cdot 2H_2O$ (s)	−2533.0	−2548.2	0.6
	Acetate Salts		
$Sr(CH_3COO)_2$ (s)	−1487.4		
$Sr(CH_3COO)_2\cdot 1/2H_2O$ (s)	−1631.8	−1636.7	0.3
$Ca(CH_3COO)_2$ (s)	−1479.5		
$Ca(CH_3COO)_2\cdot H_2O$ (s)	−1772.3	−1778.1	0.3
	Glycolate Salts		
$CH_2OH\cdot COONa$ (s)	−900.8		
$CH_2OH\cdot COONa\cdot 1/2H_2O$(s)	−1048.9	−1050.1	0.1
$CH_2OH\cdot COOK$ (s)	−907.9		
$CH_2OH\cdot COOK\cdot 1/2H_2O$ (s)	−1064.4	−1057.2	0.7
$Ca(CH_2OH\cdot COO)_2$ (s)	−1856.0		
$Ca(CH_2OH\cdot COO)_2\cdot 3H_2O$ (s)	−2736.3	−2751.8	0.6
$Ca(CH_2OH\cdot COO)_2\cdot 5H_2O$ (s)	−3311.2	−3349.0	1.1
	Sodium Disodium Hydroxyacetate		
$NaOCH_2CO_2Na$ (s)	−1037.2		
$NaOCH_2CO_2Na\cdot 2H_2O$ (s)	−1649.3	−1634.4	0.9

Table 6. Results for Linear SDR Plots for Ammoniates of Indium Trihalides, InX_3 (X = Cl, Br, I)[a]

	experimental			predictions and % errors					
	$\Delta_f H^o$	$\Delta_f H^o$	$\Delta_f H^o$	$\Delta_f H^o$		$\Delta_f H^o$		$\Delta_f H^o$	
n	X = Cl	X = Br	X = I	X = Cl	% error	X = Br	% error	X = I	% error
0	−537.2	−428.9	−238	−622.7	−15.9	−518.6	−20.9	−344.3	−44.7
1	−680.3			−714.8	−5.1	−612.9		−435.0	
2	−815.9		−497.9	−806.9	1.1	−707.1		−525.7	−5.6
3	−948.1	−829.7		−899.0	5.2	−801.3	3.4	−616.4	
5	−1148.5	−1051.4	−852.7	−1083.2	5.7	−989.7	5.9	−797.8	6.4
7	−1318	−1226.7	−1048.9	−1267.4	3.	−1178.2	4.0	−979.2	6.6
9			−1222.1	−1451.6		−1366.7		−1160.5	5.0
13			−1544	−1819.9		−1743.5		−1523.3	1.3
15	−1950	−1883		−2004.1	−2.8	−1931.9	−2.6	−1704	
21			−2176	−2556.7		−2497.2		−2248.9	−3.3

[a] Columns 2−4 list the experimentally known NBS[36] data for $\Delta_f H^o(InX_3 \cdot n NH_3, s)/kJ \cdot mol^{-1}$; columns 5, 7, and 9 give the SDR predictions for $\Delta_f H^o(InX_3 \cdot n NH_3, s)/kJ \cdot mol^{-1}$; and columns 6, 8, and 10 give the percentage errors for these predictions.

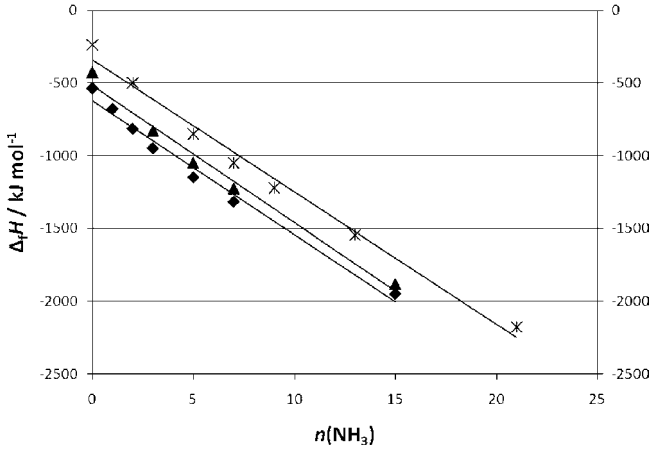

Figure 4. Plot of $\Delta_f H°(InX_3 \cdot n NH_3, s)/kJ \cdot mol^{-1}$ versus *n* for X = Cl (diamonds), Br (triangles), and I (stars) showing linear fit. See text for list of fitted linear equations.

for this system—than is obtained for the ammoniates as a family. Table 6 shows how the linear fits above reproduce the known experimental data. Reproduction of the parent data, $P(InX_3, s)/kJ \cdot mol^{-1}$, is, however, seriously different (being between 16 and 45 %) from the NBS experimental data.

Since the plots in Figure 4 have a definite curvature, one can examine a polynomial fit (degree 2). Table 7 and Figure 5 show that this provides a much improved fit and, likely, a much better prediction of the data which is missing for the various intermediate ammoniates.

The polynomial fits take the analytical form

$$\Delta_f H^o(InCl_3 \cdot n NH_3,s)/kJ \cdot mol^{-1} = 2.490n^2 - 130.1n - 554.8 \quad (\text{Diamonds}, R^2 = 0.999)$$

$$\Delta_f H^o(InCl_3 \cdot n NH_3,s)/kJ \cdot mol^{-1} = 2.422n^2 - 132.5n - 438.3 \quad (\text{Triangles}, R^2 = 0.999)$$

$$\Delta_f H^o(InCl_3 \cdot n NH_3,s)/kJ \cdot mol^{-1} = 1.379n^2 - 119.7n - 260.0 \quad (\text{Stars}, R^2 = 0.999)$$

and from these results and Table 7 we note that:

(1) correlation coefficients are considerably improved compared to those for the linear SDR plots (Figure 4);

(2) errors in reproduction of *known* data are considerably less than those in Table 6 (except in a single instance) and rarely greater than 3 %;

(3) Table 7 is anticipated to provide reliable estimates for

$\Delta_f H^o(InCl_3 \cdot n NH_3,s)$ for values of n = 4, 6, 8, 10−12, 14, 16−20, and possibly slightly beyond n = 21

$\Delta_f H^o(InBr_3 \cdot n NH_3,s)$ for values of n = 1, 2, 4, 6, 8−14

$\Delta_f H^o(InBr_3 \cdot n NH_3,s)$ for values of n = 1, 3, 4, 6, 8, 10−12, 16−20

(4) intercept terms are closer to the known[36] parent $\Delta_f H°$ values with errors of −3.3 % (X = Cl); 2.2 % (X = Br), and −9.2 % (X = I);

(5) the nonlinearity for the ammoniates with $n > 5$ or 6 corresponds to continuously decreasing solvation enthalpy. This

Table 7. Results for Quadratic SDR Plots for Ammoniates of Indium Trihalides, InX_3 (X = Cl, Br, I)[a]

	experimental			predictions and % errors					
	$\Delta_f H^o$	$\Delta_f H^o$	$\Delta_f H^o$	$\Delta_f H^o$		$\Delta_f H^o$		$\Delta_f H^o$	
n	X = Cl	X = Br	X = I	X = Cl	% error	X = Br	% error	X = I	% error
0	−537.2	−482.9	−238	−554.8	−3.3	−438.3	2.2	−260.0	−9.2
1	−680.3			−682.4	−0.3	−568.3		−378.3	
2	−815.9		−497.9	−805.1	1.3	−693.5		−493.8	0.8
3	−948.1	−829.7		−922.8	2.7	−813.9	1.9	−606.5	
5	−1148.5	−1051.4	−852.7	−1143.2	0.5	−1040.1	1.1	−823.8	3.4
7	−1318	−1226.7	−1048.9	−1343.6	−1.9	−1247.0	−1.7	−1030.0	1.8
9			−1222.1	−1524.2		−1434.4		−1225.1	−0.2
13			−1544	−1825.5		−1751.2		−1582.4	−2.5
15	−1950	−1883		−1946.3	0.2	−1880.5	0.1	−1744.5	
21			−2176	−2189.1		−22152.2		−2164.5	0.5

[a] Columns 2−4 list the experimentally known NBS[36] data for $\Delta_f H^o(InX_3 \cdot n NH_3, s)$; columns 5, 7, and 9 give the SDR predictions for $\Delta_f H^o(InX_3 \cdot n NH_3, s)$ and columns 6, 8, and 10 the percentage errors in these predictions.

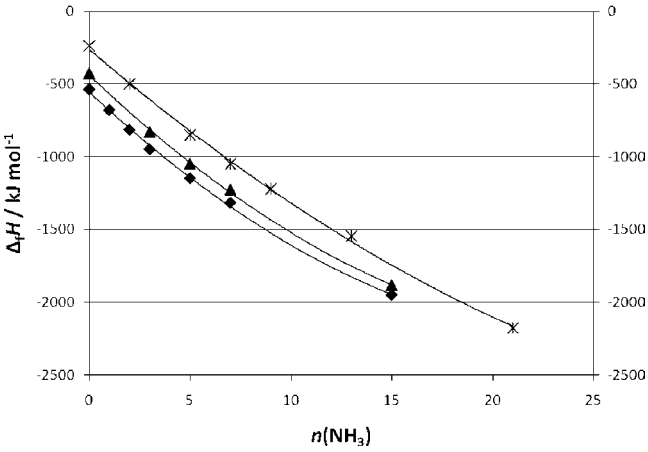

Figure 5. Plot of $\Delta_f H°(InX_3 \cdot nH_2O, s)/kJ \cdot mol^{-1}$ versus n for X = Cl (diamonds), Br (triangles), and I (stars) showing polynomial fit (degree 2). See text for list of fitted quadratic equations.

contrasts markedly with the strict additivity which we have always observed for the hydrates. The strong interactions formed by water with the local environment give rise to the linear behavior observed in hydrates.

Significantly, the ammoniates also have the largest number ($n = 21$) of solvate molecules. Since, clearly, not all of these can be coordinated to the central ion this may cause deviations at higher values of n. Thus, the curvature in ammoniates could arise from at least two sources:

• the changing environment into which successive ammonia solvates are inserted, together with the relatively weak local interactions[45] between the molecules of both ammonia and solid solvate. The minimum enthalpy of incorporation of NH_3 into the solvate is observed[44] to be $-92.3\ kJ \cdot mol^{-1}$, a value which accords exactly with the average value found here for the indium trihalide ammoniates.

• an artifact of the data since these systems do not provide easy experimental thermochemistry. It seems worthwhile to suggest an experimental program to investigate these issues.

Other systems where $L \neq NH_3$ can be handled similarly, provided data exist. Examples are given below for cases where $L = H_2S$, $(CH_3)_2S$, and SO_2.

Example 7. The NBS database[36] lists $\Delta_f H°(BeBr_2, s)/kJ \cdot mol^{-1} = -353.5$. What is the value predicted by SDR for $\Delta_f H°(BeBr_2 \cdot 2H_2S, s)/kJ \cdot mol^{-1}$?

From Table 1 in ref 4, $\theta_{Hf}(H_2S)/kJ \cdot mol^{-1} \approx -53.6$, and since $n = 2$, so from eq 11

$$\Delta_f H^o(BeBr_2 \cdot 2H_2S,s)/kJ \cdot mol^{-1} \approx -353.5 + 2(-53.6) = -460.7$$

The experimental value listed[36] is $-469\ kJ \cdot mol^{-1}$ (error 1.8 %).

Example 8. The NBS database[36] lists $\Delta_f H°(InBr_3 \cdot 2(CH_3)_2S, s)/kJ \cdot mol^{-1} = -610.4$. What is the value predicted by SDR for $\Delta_f H°(InCl_3 \cdot 2(CH_3)_2S, s)$? Can solvates other than those of $(CH)_2S$ be employed to make SDR estimates?

The solvent system $L = (CH_3)_2S$ has very few solvate examples for which data have been acquired. For this reason, making an SDR plot is not feasible. However, we can devise a plethora of various forms of eqs 12−16 inventively, to predict values for this and other solvents. Using NBS values exclusively, we have, using eq 13 in a general form

$$\Delta_f H^o(InCl_3 \cdot 2(CH_3)_2S,s) + \Delta_f H^o(InBr_3 \cdot nNH_3,s) \approx \Delta_f H^o(InBr_3 \cdot 2(CH_3)_2S,s) + \Delta_f H^o(InCl_3 \cdot nNH_3,s)$$

This equation, using values of $\Delta_f H°(InX_3 \cdot nNH_3, s)$ [X = Cl, Br] discussed earlier, leads to the following predictions for $\Delta_f H°(InCl_3 \cdot 2(CH_3)_2S, s)/kJ \cdot mol^{-1}$: −728.9 (8.1 %, $n = 3$); −707.5 (5.0 %, $n = 5$); −701.7 (4.1 %, $n = 7$); and −677.4 (0.5 %, $n = 15$). Errors and degree of solvation, n, are given in parentheses. The errors are calculated using the NBS value of $-674.0\ kJ \cdot mol^{-1}$ cited[36] for $\Delta_f H°(InCl_3 \cdot 2(CH_3)_2S, s)$.

Using eq 14 in the form

$$\Delta_f H^o(InCl_3 \cdot 2(CH_3)_2S,s) + \Delta_f H^o(InBr_3,s) \approx \Delta_f H^o(InBr_3 \cdot 2(CH_3)_2S,s) + \Delta_f H^o(InCl_3,s)$$

with parent salt data from NBS,[36] $-\Delta_f H°(InBr_3, s)/kJ \cdot mol^{-1} = -482.9$; $\Delta_f H°(InBr_3 \cdot 2(CH_3)_2S, s)/kJ \cdot mol^{-1} = -610.4$, and $\Delta_f H°(InCl_3,s)/kJ \cdot mol^{-1} = -537.2$ leads to $\Delta_f H°(InCl_3 \cdot 2(CH_3)_2S, s)$ predicted to be approximately $[-610.4 - 537.2 + 482.9] = -664.7\ kJ \cdot mol^{-1}$ (1.4 %).

A further approach, using eq 13 in the form

$$\Delta_f H^o(InCl_3 \cdot 2(CH_3)_2S,s) + \Delta_f H^o(GaBr_3 \cdot nNH_3,s) \approx \Delta_f H^o(InBr_3 \cdot 2(CH_3)_2S,s) + \Delta_f H^o(GaCl_3 \cdot nNH_3,s)$$

leads to the following results for $\Delta_f H°(InCl_3 \cdot 2(CH_3)_2S, s)/kJ \cdot mol^{-1}$: −760.7 (12.8 %, $n = 1$); −738.1 (9.5 %, $n = 5$); −730.1 (8.3 %, $n = 6$); −725.9 (7.7 %, $n = 7$); and −727.6 (8.0 %, $n = 14$).

The involvement of hydrate data might normally be expected to lead to improved results. However, trivalent halides do not form hydrates readily and data are sparse. However, we can, for example, devise an equation using eq 16 in the form

$$\Delta_f H^o(InCl_3 \cdot 2(CH_3)_2S,s) + \Delta_f H^o(MBr_3 \cdot nH_2O,s) \approx \Delta_f H^o(InBr_3 \cdot 2(CH_3)_2S,s) + \Delta_f H^o(InCl_3 \cdot nNH_3,s)$$

where M represents a trivalent metal. For thallium chloride and bromide hydrates, thermodynamic data have been reported[36] for $\Delta_f H°(TlCl_3 \cdot 4H_2O, s)/kJ \cdot mol^{-1} = -1503$ and $\Delta_f H°(TlBr_3 \cdot 4H_2O, s)/kJ \cdot mol^{-1} = -1402$. Specifically

$$\Delta_f H^o(InCl_3 \cdot 2(CH_3)_2S,s) + \Delta_f H^o(TlBr_3 \cdot 4H_2O,s) \approx \Delta_f H^o(InBr_3 \cdot 2(CH_3)_2S,s) + \Delta_f H^o(TlCl_3 \cdot 4H_2O,s)$$

and thus $\Delta_f H°(InCl_3 \cdot 2(CH_3)_2S, s)/kJ \cdot mol^{-1} \approx [-610.4 - 1503 + 1402] = -711.4$ (5.5 %).

Finally, by considering SO_2 solvates, we can give an example of eq 15 in use. We can predict data for $\Delta_f H°(AlCl_3 \cdot 2SO_2, s)/kJ \cdot mol^{-1}$ using the SDR

$$\Delta_f H^o(AlCl_3 \cdot 2SO_2,s) + \Delta_f H^o(LiI \cdot SO_2,s) \approx \Delta_f H^o(LiI \cdot 2SO_2,s) + \Delta_f H^o(AlCl_3 \cdot SO_2,s)$$

Taking[36] $\Delta_f H°(LiI \cdot SO_2, s)/kJ \cdot mol^{-1} = -607.9$; $\Delta_f H°(LiI \cdot 2SO_2, s)/kJ \cdot mol^{-1} = -944.3$; and $\Delta_f H°(AlCl_3 \cdot SO_2, s)/kJ \cdot mol^{-1} = -1061.1$ leads to $\Delta_f H°(AlCl_3 \cdot 2SO_2, s)$ predicted to be $\approx [-1061.1 - 944.3 + 607.9] = -1398.0$ which agrees exactly with the value reported.[4]

Acknowledgment

One of us (HDBJ) would like to record his pleasure and his thanks to John Rowlinson for generously giving up time to discuss aspects of thermodynamics on a 1:1 basis and for his kind hospitality shown at Carlton House Terrace.

Supporting Information Available:

Excel spreadsheets ("Solver Example.xlsx" for Excel 2007 and "Solver Example.xls" for earlier versions) demonstrate the use of Excel Solver to optimize a set of additive contributions to a thermodynamic quantity as compared with a reference set. This material is available free of charge via the Internet at http://pubs.acs.org.

Literature Cited

(1) Jenkins, H. D. B. *Chemical Thermodynamics - at a Glance*, ISBN-10: 1405139978; ISBN-13: 978-1405139977, Blackwell: Oxford, 2008.

(2) O'Hare, P. A. G. Inorganic Chalcogenides: High-tech Materials, Low-tech Thermodynamics. *J. Chem. Thermodyn.* **1978**, *19*, 675–701.

(3) Jenkins, H. D. B.; Glasser, L. Ionic Hydrates, $M_pX_q.nH_2O$: Lattice Energy and Standard Enthalpy of Formation Estimation. *Inorg. Chem.* **2002**, *41*, 4378–4388.

(4) Jenkins, H. D. B.; Glasser, L. The Difference Rule - A New Thermodynamic Principle: Prediction of Standard Thermodynamic Data for Inorganic Solvates. *J. Am. Chem. Soc.* **2004**, *126*, 15809–15817.

(5) Jenkins, H. D. B.; Liebman, J. F. Extensions and Corollaries of the Thermodynamic Solvate Difference Rule. *J. Chem. Eng. Data* **2009**, *54*, 351–358 (Invited contribution to Robin H. Stokes Festschrift Edition).

(6) Glasser, L.; Jenkins, H. D. B. The Thermodynamic Solvate Difference Rule: Solvation Parameters and their use in the Interpretation of the Role of Solvate in Solid Solvates. *Inorg. Chem.* **2007**, *46*, 9768–9778.

(7) Brownridge, S.; Calhoun, L.; Jenkins, H. D. B.; Laitinen, R. S.; Murchie, M. P.; Passmore, J.; Pietikäinen, J.; Rautinen, J.; Mikko Sanders, J. C. P.; Schrobilgen, G. J.; Suontamo, R. J.; Tuononen, H. M.; Valkonen, J. U.; Ming Wong, C. ^{77}Se NMR Spectroscopic, DFT MO and VBT Investigation of the Reversible Dissociation of Solid $(Se_6I_2)[AsF_6]_2.2SO_2$ in Liquid SO_2 to Solutions Containing 1,4-$Se_6I_2^{2+}$ in Equilibrium with Se_n^{2+} ($n = 4$, 8, 10) and Seven Binary Selenium Iodine Cations: Preliminary Evidence for 1,1,4,4-$Se_4Br_4^{2+}$ and *cyclo*-Se_7Br^+. *Inorg. Chem.* **2009**, *48*, 1938–1959.

(8) Jenkins, H. D. B.; Roobottom, H. K.; Passmore, J.; Glasser, L. Relationships among Ionic Lattice Energies, Molecular (Formula Unit) Volume and Thermochemical Radii. *Inorg. Chem.* **1999**, *38*, 3609–3620.

(9) Glasser, L.; Jenkins, H. D. B. Lattice Energies and Unit cell Volumes of Complex Ionic Solids. *J. Am. Chem. Soc.* **2000**, *122*, 632–638.

(10) Jenkins, H. D. B.; Tudela, D.; Glasser, L. Lattice Potential Energy Estimation for Complex Ionic Salts from Density Measurements. *Inorg. Chem.* **2002**, *41*, 2364–2367.

(11) Marcus, Y.; Jenkins, H. D. B.; Glasser, L. Ion Volumes: a Comparison. *J. Chem. Soc., Dalton Trans.* **2002**, 3795–3798.

(12) Jenkins, H. D. B.; Glasser, L. Standard Absolute Entropy, Values from Volume and Density. 1. Inorganic Materials. *Inorg. Chem.* **2003**, *42*, 8702–8708.

(13) Jenkins, H. D. B.; Tudela, D. New Methods to Estimate Lattice Energies. *J. Chem. Educ.* **2003**, *80*, 1482–1487.

(14) Glasser, L.; Jenkins, H. D. B. Standard Absolute Entropy, Values from Volume and Density. 2. Organic Materials. *Thermochim. Acta* **2004**, *414*, 125–130.

(15) Jenkins, H. D. B. Thermodynamics of the Relationship between Lattice Energy and Lattice Enthalpy. *J. Chem. Educ.* **2005**, *82*, 950–952.

(16) Jenkins, H. D. B.; Glasser, L.; Klapötke, T. M.; Crawford, M.-J.; Bhasin, K. K.; Lee, J.; Schrobilgen, G. J.; Sunderlin, L.; Liebman, J. F. The Ionic Isomegethic Rule and Additivity Relationships: Estimation of Ion Volumes. A Route to Energetics and Entropics of New, Traditional, Hypothetical and Counterintuitive Materials. *Inorg. Chem.* **2004**, *43*, 6238–6248.

(17) Glasser, L.; Jenkins, H. D. B. Predictive Thermodynamics for Condensed Phases. *Chem. Soc. Rev.* **2005**, *34*, 866–874.

(18) Jenkins, H. D. B.; Liebman, J. F. Volumes of Solid State Ions and their Estimation. *Inorg. Chem.* **2005**, *44*, 6359–6372.

(19) Jenkins, H. D. B.; Glasser, L. Volume Based Thermodynamics - Estimations for 2:2 Salts. *Inorg. Chem.* **2006**, *45*, 1754–1756.

(20) Jenkins, H. D. B.; Glasser, L. Internally Consistent Ion Volumes and Their Application in Volume-Based Thermodynamics. *Inorg. Chem.* **2008**, *47*, 6195–6202.

(21) Glasser, L.; Jenkins, H. D. B. Volume-Based Thermodynamics (VBT): A Prescription for Application and Usage to Approximate Thermodynamic Data. *J. Chem. Eng. Data* **2011**, to be submitted October 2010 (Invited contribution to Robin Prausnitz Festschrift Edition).

(22) Roux, M. V.; Davalos, J. Z; Jimenez, P.; Notario, R.; Castano, O.; Chickos, J. S.; Hanshaw, W.; Zhao, H.; Rath, N.; Liebman, J. F.; Farivar, B. S.; Bashir-Hashemi, A. Cubane, cuneane and their carboxylates: a calorimetric, crystallographic, calculational and conceptual coinvestigation. *J. Org. Chem.* **2005**, *70*, 5461–5470.

(23) Fattahi, A.; Kass, S. R.; Liebman, J. F.; Matos, M. A. R.; Miranda, M. S.; Morais, V. M. F. The enthalpies of formation of o-, m-and p-benzoquinone: gas-phase ion energetics, combustion calorimetry and quantum chemical computations combined. *J. Am. Chem. Soc.* **2005**, *127*, 6116–6122.

(24) Emel'yanenko, V. N.; Verevkin, S. P.; Heintz, A. The gaseous enthalpy of formation of the ionic liquid 1-butyl-3-methylimidazolium dicyanamide from combustion calorimetry, vapor pressure measurements and ab initio calculations. *J. Am. Chem. Soc.* **2007**, *129*, 3930–3937.

(25) Rustad, J. R.; Nelmes, S. L.; Jackson, V. E.; Dixon, D. A. Quantum-chemical calculations of carbon-isotope fractionation in CO_2(g), aqueous carbonate species and carbonate minerals. *J. Phys. Chem. A* **2008**, *112*, 542–555.

(26) Klapötke, T. M.; Krumm, B.; Ilg, R.; Troegel, D.; Tacke, R. The sila-explosives $Si(CH_2N_3)_4$ and $Si(CH_2ONO_2)_4$: silicon analogues of the common explosives pentaerythrityl tetraazide, $C(CH_2N_3)_4$, and pentaerythritol tetranitrate, $C(CH_2ONO_2)_4$. *J. Am. Chem. Soc.* **2007**, *129*, 6908–6915.

(27) Gao, H.; Ye, C.; Piekarski, C. M.; Shreeve, J. M. Computational characterization of energetic salts. *J. Phys. Chem. C* **2007**, *111*, 10718–1073.

(28) Steele, W. V.; Chirico, R. D.; Knipmeyer, S. E.; Nguyen, A. Thermodynamic properties and ideal-gas enthalpies of formation for trans-methyl cinnamate, α-methyl cinnamaldehyde, methyl methacrylate, 1-nonyne, trimethylacetic acid, trimethylacetic anhydride and ethyl trimethyl acetate. *J. Chem. Eng. Data* **2002**, *47*, 700–714.

(29) Xu, X.-G.; Zeng, Z.-X.; Xue, W.-L.; Zhang, H.-Y. Heat capacity and enthalpy of formation of trimethyl phosphite, 2-chloromethylbenzonitrile and 2-dimethylphosphonomethylbenzonitrile. *J. Chem. Eng. Data* **2007**, *52*, 1189–1194.

(30) Dibrivnyi, V. N.; Mel'nik, G. V.; Van-Chin-Syan, Yu.Ya.; Yuvchenko, A. P. The thermodynamic properties of four triphenylsilane acetylene peroxides. *Russ. J. Phys. Chem.* **2006**, *80*, 330–334.

(31) Verevkin, S. P. Improved Benson increments for the estimation of standard enthalpies of formation and enthalpies of vaporization of alkyl ethers, acetals, ketals and orthoesters. *J. Chem. Eng. Data* **2002**, *47*, 1071–1097.

(32) Benson, S. W.; Buss, J. H. Additivity Rules for the Investigation of Molecular Properties. *J. Chem. Phys.* **1958**, *29*, 546–572.

(33) Da Silva, G.; Bozzelli, J. W. Thermochemistry, Bond Energies, and Internal Rotor Potentials of Dimethyl Tetraoxide. *J. Phys. Chem. A* **2007**, *111*, 12026–12036.

(34) Benson, S. W. *Thermochemical Kinetics*, 2nd ed.; John Wiley: New York, 1976.

(35) Fyfe, W. S.; Turner, F. J.; Verhoogen, J. Metamorphic Reactions and Metamorphic Facies. *Geol. Soc. Am., Memoir* **1958**, 73.

(36) Wagman, D. D.; Evans, W. H.; Parker, V. B.; Schumm, R. H.; Halow, I.; Bailey, S. M.; Churney, K. L.; Nuttall, R. L. *Journal of Physical and Chemical Reference Data: The NBS Tables of Chemical Thermodynamic Properties. Selected Values for Inorganic and C1 and C2 Organic Substances in SI Units*; 1982, 1−392; Vol. 11, Suppl. No. 2.

(37) Chase, M. W. *J. Phys. Chem. Ref. Data, Monogr.*, 4th ed. NIST-JANAF Thermochemical Tables, 1998; Vol. 9.

(38) Latimer, W. M. *Oxidation Potentials*, 2nd ed.; Prentice Hall: Englewood Cliffs, N. J., 1961.

(39) Latimer, W. M. Methods of Estimating the Entropies of Solid Compounds. *J. Am. Chem. Soc.* **1951**, *72*, 1480–1482.

(40) Karapet'yants, M. Kh.; Karapet'yants, M. L. *Thermodynamic Constants of Inorganic and Organic Compounds*; Schmorak, J., transl.; Ann Arbor-Humphrey Science Publications: Ann Arbor, London, 1970.

(41) Berg, L. G.; Pribylov, K. B. Heat effects in the dehydration of $MgSO_4 \cdot 7H_2O$. *Zhur. Neorg. Khim.* **1965**, *10*, 1419–1422.

(42) Schneider, V. A. Doctoral Thesis, M. Kh. T. im D. I. Mendeleeva, 1958.

(43) Selivanova, N. M.; Shneider, V. A. Heat of formation of $MgSeO_4$ from elements. *Zhur. Neorg. Khim.* **1961**, *6*, 27–33.

(44) Glasser, L.; Jones, F. Systematic Thermodynamics of Hydration (and of Solvation) of Inorganic Solids. *Inorg. Chem.* **2009**, *48*, 1661–1665.

(45) Nelson, D. D., Jr.; Fraser, G. T.; Klemperer, W. Does Ammonia Hydrogen Bond? *Science* **1987**, *238*, 1670–1674.

Received for review April 20, 2010. Accepted May 17, 2010.

JE100383T